A Probability Hypothesis Density-Based Multitarget Tracker Using Multiple Bistatic Range and Velocity Measurements

Martin Tobias and Aaron D. Lanterman
School of Electrical and Computer Engineering
Georgia Institute of Technology
Atlanta, Georgia 30332–0250 U.S.A.
mtobias@ece.gatech.edu, lanterma@ece.gatech.edu

Keywords— Multitarget Tracking, Probability Hypothesis Density, Passive Radar, Sensor Fusion, Passive Coherent Location.

Abstract— A novel multitarget tracking scheme for passive radar, using a particle filter implementation of Ronald Mahler's Probability Hypothesis Density (PHD), is presented. Using range and velocity measurements from a simple non-directional receive antenna and low frequency transmitter pair, a target can be located along an ellipse. To pinpoint a target, multiple such antenna pairs are needed to locate the target at the intersection of the corresponding ellipses. Determining the intersection of these bistatic range ellipses, and resolving the resultant ghost targets, is generally a complex task. However, the PHD is found to provide a convenient and simple means of fusing together the multiple range and velocity measurements into coherent target tracks.

I. Introduction

Passive radars, such as Lockheed Martin's *Silent Sentry*® system, have a number of advantages over conventional active radar, including covert operation and lower cost, since a passive radar system exploits "illuminators of opportunity," such as FM radio and TV transmissions, which already exist. However, the low frequencies involved in using the "illuminators of opportunity" make it difficult to accurately measure bearing information. We therefore consider tracking targets with just range and velocity measurements. To achieve this, we implement a particle-filter application of Ronald Mahler's Probability Hypothesis Density (PHD) to multitarget tracking using simulated passive radar data.

II. Passive Coherent Location

Target Range

Using a passive radar receiver and an independent transmitting antenna, a target can be located along an ellipse determined by:

$$R = \sqrt{(x-x_t)^2 + (y-y_t)^2} + \sqrt{(x-x_r)^2 + (y-y_r)^2} \tag{1}$$

where (x_r, y_r) and (x_t, y_t) are the locations of the antennas, and (x, y) is the location of the target. The antennas are located at the foci of the ellipse.

To resolve a target's location, multiple such transmitter-receiver pairs are needed, allowing the target to be tracked at the intersection of the resulting ellipses. Figure 2 shows an example of these range ellipses.

Target Velocity

The passive radar system also measures a target's velocity in terms of the rate of change of the range measurement:

$$V = \frac{(x-x_r)\dot{x} + (y-y_r)\dot{y}}{\sqrt{(x-x_r)^2 + (y-y_r)^2}} + \frac{(x-x_t)\dot{x} + (y-y_t)\dot{y}}{\sqrt{(x-x_t)^2 + (y-y_t)^2}} \tag{2}$$

III. The Probability Hypothesis Density (PHD)

Ronald Mahler introduced the concept of a probability hypothesis density, which is defined as being any function that, when integrated over any given area, specifies the expected number of targets present in that area. More specifically, the PHD is the factorial moment density found in point process theory, and it provides a straightforward method of estimating the number of targets in the region under observation. Using probability generating functionals and set calculus, Mahler derives Bayesian time-update and data-update equations that use the PHD to perform motion prediction and incorporate radar observations, respectively [1–4].

The PHD Time-Update equation is given by:

$$\hat{D}_{k+1|k}(\mathbf{y}|Z^{(k)}) = \hat{b}_{k+1|k}(\mathbf{y}) + \int \Big(d_{k+1|k}(\mathbf{y}) f_{k+1|k}(\mathbf{y}|\mathbf{x}) + \hat{b}_{k+1|k}(\mathbf{y}|\mathbf{x}) \Big) \hat{D}_{k|k}(\mathbf{x}|Z^{(k)}) dx \tag{3}$$

where $f_{k+1|k}(\mathbf{y}|\mathbf{x})$ is the single-target motion model's Markov transition density; $d_{k+1|k}(\mathbf{y})$ is the probability that the target at state $\mathbf{y}$ at time k will *not* disappear at time $k+1$; $\hat{b}_{k+1|k}(\mathbf{y}|\mathbf{x})$ is the PHD of $b_{k+1|k}(Y|\mathbf{x})$, which is the multitarget likelihood density function of a target with state $\mathbf{x}$ at time k spawning a set of new targets Y at time $k+1$; and $\hat{b}_{k+1|k}(\mathbf{y})$ is the PHD of $b_{k+1|k}(Y)$, which is the likelihood function that a set of new targets Y will be born spontaneously at time $k+1$. The ˆ symbol above a variable indicates that it is a PHD.

Assuming statistically independent target motion, the PHD Data-Update equation is approximated by:

$$\hat{D}_{k+1|k+1}(\mathbf{x}|Z^{(k+1)}) \cong \alpha_0 \, \hat{D}_{k+1|k}(\mathbf{x}|Z^{(k)}) + \sum_{\mathbf{z}\in Z_{k+1}} \alpha_i \, \hat{D}_{k+1|k+1}(\mathbf{x}|\mathbf{z}, Z^{(k)}) \quad (4)$$

where:

$$\alpha_0 = 1 - p_D \, ,$$

$$\alpha_i = \frac{p_D \hat{D}_{k+1}(\mathbf{z}_i|Z^{(k)})}{\lambda_{k+1} c_{k+1}(\mathbf{z}) \; + \; p_D \hat{D}_{k+1}(\mathbf{z}_i|Z^{(k)})} \, ,$$

$$\hat{D}_{k+1}(\mathbf{z}|Z^{(k)}) = \int f(\mathbf{z}|\mathbf{x}) \hat{D}_{k+1|k}(\mathbf{x}|Z^{(k)}) dx \, ,$$

and

$$\hat{D}_{k+1|k+1}(\mathbf{x}|\mathbf{z}, Z^{(k)}) = \frac{f(\mathbf{z}|\mathbf{x}) \hat{D}_{k+1|k}(\mathbf{x}|Z^{(k)})}{\hat{D}_{k+1}(\mathbf{z}|Z^{(k)})}.$$

$Z_{k+1} = \{z_1, z_2, ...\}$ is the set of observations collected by the sensor at time $k+1$. $f(\mathbf{z}|\mathbf{x})$ is the single-target likelihood function of the sensor. The probability of detection is given by p_D. The false-alarm rate is assumed to be Poisson distributed with parameter λ_{k+1} and density $c_{k+1}(\mathbf{z})$.

By integrating the data-updated PHD, and rounding to the nearest integer, we find the expected number of targets at time $k+1$. That is,

$$N_{k+1|k+1} = \int \hat{D}_{k+1|k+1}(\mathbf{y}|Z^{(k+1)}) dx \quad (5)$$

and

$$\tilde{N} = E[no. \; of \; targets] = [N_{k+1|k+1}]_{nearest \; integer.} \quad (6)$$

The location of the targets is found by extracting the location of the $\tilde{N}$ highest peaks of the data-updated PHD.

IV. Particle Filter Implementation

We implement a particle-filter version of the PHD filtering equations. The particles track the x and y coordinates of the targets, as well as the x and y components of the target velocities. During each time-step, the particles undergo time-updating, data-updating, peak-extraction, and resampling.

Initialization

In our simulation, the particle filter is initialized with $1{,}000$ particles. Each particle is placed at a uniformly random location within the field of view (FoV). The FoV is chosen to be rectangular and of size 100×100. The velocity parameters of each particle are also chosen randomly over a finite uniform distribution. Before simulation begins, the filter must assume that there is at least one target present, and so the PHD over the FoV must initially sum to one. Hence, the particles are identically weighted with $w_i = 1/(no. particles)$, such that

$$\sum_i w_i = 1. \quad (7)$$

If in fact no targets are present, the expected number of targets, as found in (6), will be zero after the first iteration of the filter.

Time Update

During the time-update step, the particles are propagated according to a simple target motion model, and uniform process noise is added. Additional particles are also added to the filter according to a birth model that accounts for the entrance of new targets into the FoV. In our simulation, the birth model consists of 400 particles distributed uniformly along the edges of the FoV, each with randomly initialized velocities.

Data Update

During the data-update step, the passive radar range and velocity measurements are incorporated into the particle filter. Given m observations, the following weighting, w_i, which was modified from (4) by Zajic and Mahler [5] to work for particle filters, is then applied to the particles:

$$w_i = (\sum_{n=1}^{m} u_{i,n}) + \frac{M(1-p_D)}{N} \quad (8)$$

where

$$u_{i,n} = \frac{M p_D f(z_n|x_i)}{N \lambda_k c_k(z_n) \; + \; M p_D \sum_{j=1}^{N} f(z_n|x_j)} \quad (9)$$

for $i = 1, \ldots, N$. N is the total number of particles; M is the expected number of targets after the time-update step; x_i are the particles, and z_n are the observations at the current iteration. The range observations are assumed to be independent of the velocity measurements when computing the observation likelihoods, $f(z_n|x_i)$. Errors in range and velocity measurements are assumed to be normally distributed.

Peak Extraction

After the data-update step, the weights of the particles are then summed to determine the expected number of targets in the FoV. To find the target locations, an expectation-maximization (EM) algorithm [6], which we modify to account for the particle weights, is used to find the best fitting mixture of Gaussians. The algorithm to find $\theta_k = (\alpha_k, \mu_k, \Sigma_k)$, which are the weight, mean, and covariance parameters of the k-th Gaussian distribution is given by the iteration:

<u>Expectation:</u>

$$P(k|x_i) = \frac{p(x_i|\theta_k)\alpha_k}{\sum_{j=1}^{K} p(x_i|\theta_j)\alpha_j}, \quad (10)$$

Maximization:

$$\alpha_k^{new} = \sum_{i=1}^{N} w_i P(k|x_i), \tag{11}$$

$$\mu_k^{new} = \frac{1}{\alpha_k^{new}} \sum_{i=1}^{N} w_i P(k|x_i) x_i,$$

$$\Sigma_k^{new} = \frac{1}{\alpha_k^{new}} \sum_{i=1}^{N} w_i P(k|x_i)(x_i - \mu_k^{new})(x_i - \mu_k^{new})^T,$$

where K is the number of Gaussians present.

The μ_k are initialized by randomly choosing K particles and selecting their components to be the values for the μ_k. To obtain good results from the EM algorithm [7], short runs of the algorithm are performed, and the run that produces the maximum likelihood is then used for a longer EM run. The result is our final estimate of the K-Gaussian mixture. When iterating the EM algorithm, a run is terminated upon achieving a given threshold or if a covariance matrix becomes singular. The preceding is performed multiple times for different values of K, and the following minimum description length (MDL) criterion is then used to select the best fitting Gaussian mixture [8]:

$$MDL = L(\mathbf{x}; \theta_K) - \frac{\rho}{2} \ln N \tag{12}$$

where $\rho = (K-1) + K(d + d(d+1)/2)$, where d is the particle dimensionality (in our case, $d = 4$), and where

$$L(\mathbf{x}; \theta_K) = \frac{N}{\sum w_i} \sum_{i=1}^{N} w_i \ln \sum_{j=1}^{K} \alpha_j \mathcal{N}(\mu_j, \Sigma_j) \tag{13}$$

The means of the highest-weighted Gaussians in the mixture are then taken to be the expected locations and velocities of the targets. A benefit of using the EM algorithm is that we now also have covariance matrices that provide us a measure of uncertainty in our location and velocity estimates.

Resampling

Before commencing the next iteration of the PHD particle filter, the particles are resampled according to a Monte-Carlo technique. The result is a collection of 1,000 equally weighted particles, such that

$$\sum_i w_i = N_{k+1|k+1} \tag{14}$$

where $N_{k+1|k+1}$ is as in (5).

V. Preliminary Results

Our simulation consists of two targets, which are observed by a receiver via three transmitting antennas. The receiving antenna is located at $(35, 35)$, while the transmitting antennas are at $(30, 35)$, $(60, 60)$, and $(23, 12)$. The first target enters at time $k = 7$ at location $(1, 30)$ and propagates to the right with constant velocity $v = [1, 0]$. The second enters at time $k = 9$ from location (43,1) and travels up the FoV with constant velocity $v = [0, 1]$. The system parameters were chosen to facilitate our initial explorations of the PHD concept; we have not yet tried to match our parameters to the physics of any real system. That will be part of our future work.

The simulation does not include any spawning of new targets from existing targets, the existing targets are assumed not to disappear in the middle of the FoV, and their p_D is 0.99. Furthermore, no false alarms are present, and no noise is added to the radar observation measurements, so that we may test the PHD particle filter's performance under best case conditions.

Figure 1 displays the true location of the targets versus the expected values computed via the PHD filter and EM algorithm. Both range and velocity measurements were used during the PHD filtering, and the Gaussian mixture is fitted to the full particle data, namely $(x, y, \dot{x}, \dot{y})$.

We find the PHD to provide a convenient and simple means of fusing together the multiple radar measurements, so that the target locations and velocities are easily estimated without having explicitly to keep track of all the ghost targets. Figure 2 contains examples from the simulation. During time $k = 7$, the one target present is correctly detected. During time $k = 77$, two targets are correctly detected and their locations and velocities correctly estimated.

The PHD filter and EM algorithm perform well; however, we observe that they are troubled by the following:

- When the targets are located far from the antenna pairs, the corresponding range ellipses intersect with the birth particles on the edge of the FoV. This causes spurious peaks in the PHD that lead the EM algorithm to produce incorrect target estimates. See Figure 3(d) for an example of these birth-particle induced peaks.
- Ghost targets, which are caused by the ellipse intersections where no targets are present, generally disappear as the PHD filter iterates over updated radar observations. However, in the case of more than one target, range ellipses may start to overlay each other for substantial periods of time. This causes a broad ridge in the PHD, which leads to an incorrect prediction of target location. Having the transmitting antennas closer to the receiving antenna appears to exacerbate the problem in our particular simulation, and Figure 3 shows this ridging effect in the PHD when the antennas are positioned closer to each other. This scenario leads to the poor target location estimates seen in the plot on the bottom in Figure 1. The PHD filter appears to fare poorer the farther away the targets are from the antenna pairs. All of this is consistent with a well-known fact about passive radar systems, namely

that performance is highly dependent on system geometry.

VI. FUTURE WORK

- Additional antenna configurations will be tested. This includes adding more transmitting, as well as more receiving, antennas.
- Additional target configurations will be tested. The number of targets appearing and disappearing have yet to be varied. Various flight patterns, including a variety of velocities and accelerations, must also be simulated.
- Coarse direction of arrival measurements will be introduced into the simulation. This may help alleviate the PHD ridging problem caused by the range ellipses.
- A different birth model, which takes into account more realistic fields of view, will be considered.
- Finally, false alarms and lower probabilities of detection remain to be simulated, as well.

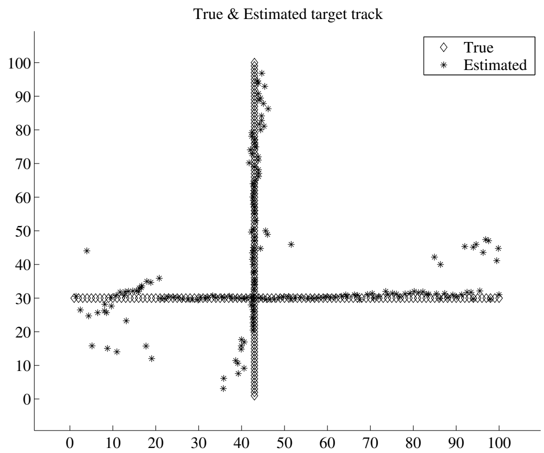

(a)

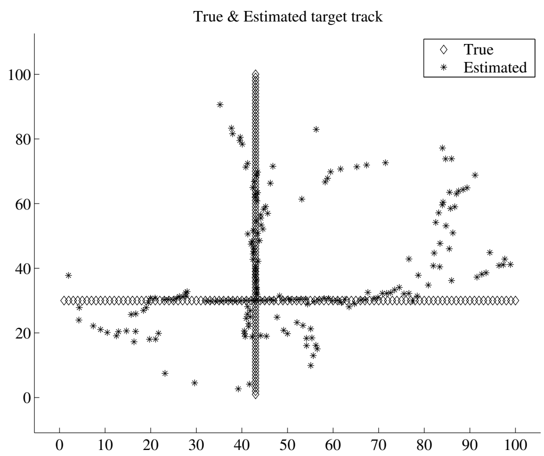

(b)

Figure 1. Estimated vs. Actual target locations. The transmitters were located closer together for the simulation on the bottom.

REFERENCES

[1] R. Mahler, "Multitarget moments and their application to multitarget tracking," in *Proc. of The Workshop on Estimation, Tracking, and Fusion: A Tribute to Yaakov Bar-Shalom*, Monterey, CA, May 2001, pp. 134–166.

[2] R. Mahler and T. Zajic, "Multitarget filtering using a multitarget first-order moment statistic," in *Signal Processing, Sensor Fusion, and Target Recognition X*, I. Kadar, Ed., vol. SPIE Proc. 4380, 2001, pp. 184–195.

[3] A. El-Fallah, T. Zajic, R. Mahler, B. Lajza-Rooks, and R. Mehra, "Multitarget nonlinear filtering based on spectral compression and probability hypothesis density," in *Signal Processing, Sensor Fusion, and Target Recognition X*, I. Kadar, Ed., vol. SPIE Proc. 4380, 2001, pp. 207–216.

[4] R. Mahler, "Objective functions for bayesian control-theoretic sensor management, i: Multitarget first-moment approximation," in *Proc. of IEEE Aerospace Conference*, vol. 4, Big Sky, MT, March 2003, pp. 1905–1924.

[5] T. Zajic and R. Mahler, "A particle-systems implementation of the phd multitarget tracking filter," in *Signal Processing, Sensor Fusion, and Target Recognition XII*, I. Kadar, Ed., vol. SPIE Proc. 5096, 2003, pp. 291–299.

[6] J. A. Bilmes, "A gentle tutorial of the em algorithm and its application to parameter estimation for gaussian mixture and hidden markov models," International Computer Science Institute, Berkeley, CA, Tech. Rep. TR-97-021, April 1998.

[7] C. Biernacki, G. Celeux, and G. Govaert, "Choosing starting values for the em algorithm for getting the highest likelihood in multivariate gaussian mixture models," *Computational Statistics and Data Analysis*, vol. 41, pp. 561–575, Jan. 2003.

[8] M. A. T. Figueiredo, J. M. N. Leitao, and A. K. Jain, "On fitting mixture models," in *Energy Minimization Methods in Computer Vision and Pattern Recognition*, E. Hancock and M. Pellilo, Eds. Springer-Verlag, 1999, pp. 54–69.

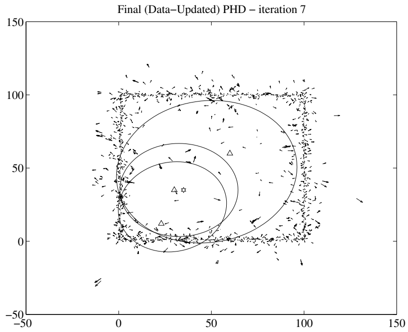

(a)Time $k = 7$. Estimated target location: $(1.43, 30.52)$, Actual target location: $(1.0, 30.0)$

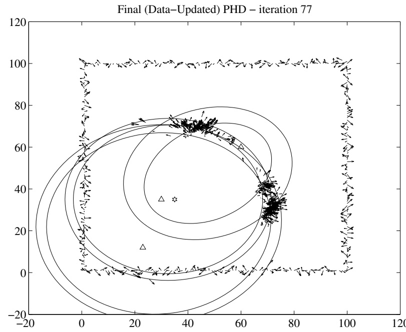

(b)Time $k = 77$. Estimated target locations: $(70.79, 30.06)$, $(42.94, 69.06)$, Actual target locations: $(71.0, 30.0)$, $(43.0, 69.0)$

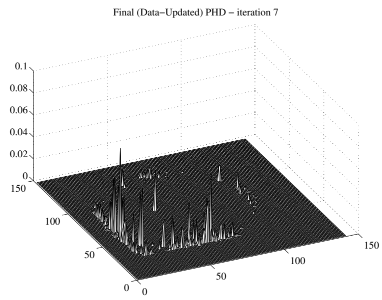

(c)The particle weights at time $k = 7$.

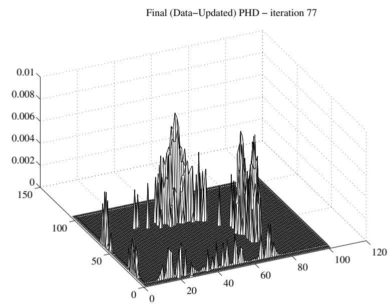

(d)The particle weights at time $k = 77$.

Figure 2. The PHD particle filter and range ellipses. The hexagon represents the location of the receiving antenna, while the triangles represent the transmitting antennas. Each particle is pictured as a vector, corresponding to its $(\dot{x}, \dot{y})$ components. Note the random velocities of the birth particles, which appear as a rectangle along the edge of the FoV. The 3-D plots display the particle weights of the PHD filter.

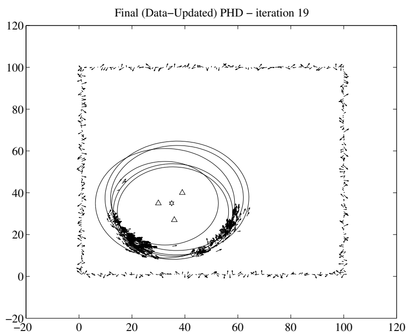

(a)Time $k = 19$. Estimated target locations: $(19.74, 18.05)$, $(55.09, 21.25)$, Actual target locations: $(13.0, 30.0)$, $(43.0, 11.0)$

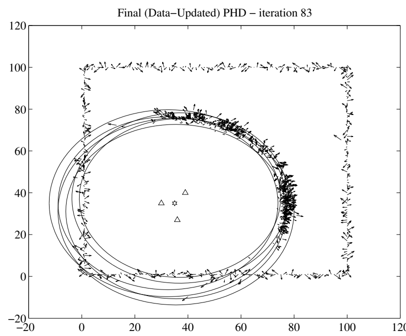

(b)Time $k = 83$. Estimated target locations: $(76.64, 32.23)$, $(58.79, 67.83)$, Actual target locations: $(77.0, 30.0)$, $(43.0, 75.0)$

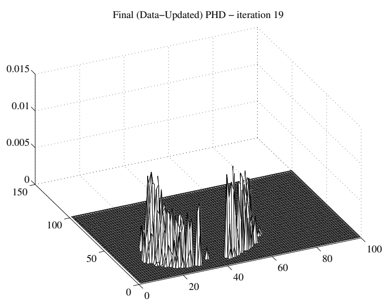

(c)The particle weights at time $k = 19$

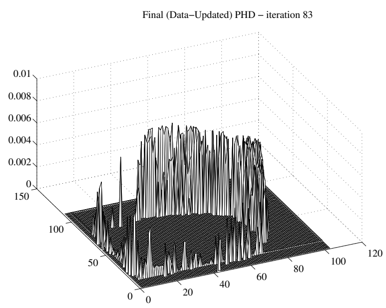

(d)The particle weights at time $k = 83$

Figure 3. The PHD particle filter and range ellipses for the case where the antenna pairs are closer together. The overlaying of the ellipses causes poor estimation of the target locations.